Ecological Indicators 146 (2023) 109847

Contents lists available at ScienceDirect

Ecological Indicators

journal homepage: www.elsevier.com/locate/ecolind

Changes in multiple ecosystem services and their influencing factors in Nordic countries

Xiangping Hu [a,*], Yanzhen Hou [b], Dan Li [c], Ting Hua [b], Maurizio Marchi [d], Johana Paola Forero Urrego [a], Bo Huang [a,*], Wenwu Zhao [b], Francesco Cherubini [a]

[a] Industrial Ecology Program, Department of Energy and Process Engineering, Norwegian University of Science and Technology, N-7491 Trondheim, Norway
[b] State Key Laboratory of Earth Surface Processes and Resource Ecology, Faculty of Geographical Science, Beijing Normal University, Beijing 100875, China
[c] State Key Laboratory of Water Resources and Hydropower Engineering Science, Wuhan University, No. 299 Bayi Street, Wuhan 430072, Hubei, China
[d] CNR – Institute of Biosciences and Bioresources, Florence Research Area, I-50019 Sesto Fiorentino, Italy

ARTICLE INFO

Keywords:
Ecosystem services
Influencing factors
Climate change
Synergies and tradeoffs
Boreal forest

ABSTRACT

Understanding changes of ecosystem services and their influencing factors is crucial for more sustainable ecosystem management and conservation of nature contributions to people, especially in regions suffering high pressure from climate change and human activities, such as the Nordic countries. In this study, we assess multiple ecosystem services and their influencing factors in Denmark, Finland, Norway, and Sweden. We analyze changes in ecosystem services such as habitat quality, sediment retention, water yield, carbon sequestration, crop and roundwood production between 2003 and 2018. The relationships between ecosystem services and the main influencing factors (temperature, precipitation, elevation, population, livestock, and land use change) are assessed by means of the Spearman's correlation coefficient and a new method that unravels synergies or tradeoffs at a grid level. Given the importance of forest management in the study region, an advanced land cover dataset that includes maps of forest harvest is produced and used as a basis for the analysis. Results show the large changes in ecosystem services during the study period and their spatial variations. Overall, the habitat quality is decreased, especially in the sites affected by forest management and agricultural production. Water yield and sediment retention increased due to higher precipitation (mainly in Norway). Higher temperature and forest management have generally increased carbon sequestration and provisioning services. The relationship between ecosystem services and their potential influencing factors differs across space. There are 10 out of 15 pairs of ecosystem services that predominantly show a tradeoff relationship, while the rest shows a synergy. In general, our results show the importance to monitor ecosystem services and understand the main drivers of their changes, so to design more sustainable resource management strategies that can secure a long-term delivery of ecosystem services.

1. Introduction

Nature ecological processes provide valuable ecosystem services (ESs) to humanity. These services are typically divided into supporting, provisioning, regulating, and culture services (Millennium ecosystem assessment, 2005). Sustainable natural resource management to maintain and restore ESs is a challenge, especially under a changing climate (Bradford and D'Amato, 2012, Rounsevell et al., 2018). With increasing population and better living standards, the implicit demand for ESs from our society is also increasing, which in turn creates additional pressure to identify successful strategies to maintain and improve ESs. In recent years, research efforts to understand status and changes of ESs have been expanding with the aim to increase the scientific evidence for sustainable ES management (Samhouri et al., 2010, Liu et al., 2022, Feng et al., 2021, Yin et al., 2021).

ESs are frequently complexly interlinked (Bennett et al., 2009, Hou et al., 2021) and their relationships are usually assessed and interpreted in terms of synergies, tradeoffs or independency (Bennett et al., 2009, Haase et al., 2012, McElwee et al., 2020). A synergy is when one service improves, and the other service also improves. A tradeoff is when one service improves while the other declines. When the change of one service has no apparent relationship with the other service, the ESs are

* Corresponding authors.
E-mail addresses: Xiangping.Hu@ntnu.no (X. Hu), Bo.Huang@ntnu.no (B. Huang).

https://doi.org/10.1016/j.ecolind.2022.109847
Received 10 August 2022; Received in revised form 15 December 2022; Accepted 27 December 2022

independent. This approach facilitates the possibility to identify management options that co-deliver across multiple ESs, or the pre-identification of the potential tradeoffs for their possible early mitigation (Dickie et al., 2011, Feng et al., 2020, Bradford and D'Amato, 2012). The relationship between ESs can have spatial heterogeneity (Turner et al., 2013). Two ESs can have a synergy relationship in one region but a tradeoff in another region (Hou et al., 2021). For instance, the synergistic effects among providing services are found to vary across Mediterranean islands (Lorilla et al., 2018), or the Tibetan Plateau of China (Hou et al., 2021). It is thus necessary to conduct site-specific analyses at high resolution to understand dynamics and spatial changes in ESs.

Nordic countries, namely Denmark, Finland, Norway, and Sweden, are a sensitive region to environmental changes since they are experiencing the highest rates of global warming and high levels of human pressure (IPCC, 2019). Human activities and climate change lead to large changes in soil erosion (SE) and land cover disturbances in this region (Zhou et al., 2021). The high rates of global warming in Nordic region affect ecosystem dynamics such as elevation of the tree lines (Bryn and Potthoff, 2018), changes in crop yields (Wiréhn, 2018), forest growth rates (Creed et al., 2015), greening of bare and mountainous areas (Myers-Smith et al., 2020), and drying of wetland (Werner et al., 2013, Zhou et al., 2021). A large part of Nordic countries is covered by forests, especially in Finland, Norway and Sweden (FAO, 2020), and the majority are managed forests periodically harvested (Ceccherini et al., 2020, Hu et al., 2018, Iordan et al., 2018). Intensive forest management and farming increased in the region, as well as urban areas and agricultural land (Zhou et al., 2021). However, the associated effects on ESs associated with these dynamics are still unclear.

There is a little number of studies on the interactions among multiple ESs in Nordic countries. Turner et al. (2014) investigated multiple ESs aiming to describe their spatial distributions and relationships, but the study only covered Denmark at a relatively coarse resolution (10 km grid) and did not assess how ESs varied over time. Queiroz et al. (2015) mapped and quantified the distribution of ESs in Sweden, but the study only covered one basin with 62 municipalities and did not assess how these ESs changed over time. Filyushkina et al. (2016) conducted a systematic review of the relationship between forest management and non-market ecosystem services, and investigated their roles in decision support models in the Nordic region. In general, existing studies focus on a limited number of ESs, and they do not assess how they vary over time, or take a coarse resolution (when not focusing on a particular region within a country). To the best of our knowledge, a comprehensive study mapping the variability in key ESs in Nordic countries within a consistent framework, with an assessment of the main drivers of a change and the relationships among ESs in terms of co-benefits and tradeoffs, is missing.

Our study aims to cover this knowledge gap by integrating gridded historical data of climatic variables with the best available datasets of ESs in Norway, Sweden, Finland, and Denmark. The analysis investigates changes and relationships of multiple ESs: habitat quality (HQ), sediment retention (SR), water yield (WY), carbon sequestration (CS), crop production (CP) and roundwood production (WP). According to the Millennium ecosystem assessment (2005), HQ is a supporting service, SR, WY, CS are regulating services and CP and WP are provisioning services. For WP and CP, spatially explicit datasets at high resolution were not available, and they have been created by combining national statistics with remote sensing data. For each grid cell, the analysis explores how each ES and influencing factor changed over time (from 2003 to 2018), the relationship between the ES and the influencing factor, and the tradeoffs or synergies between each pair of ESs. The investigated potential influencing factors are precipitation (PR), temperature (TE) at 2 m height, elevation (EL), population density (PD), livestock (LS), and changes in land cover, mainly forest (FOR) and agriculture (AGR). We use the Spearman's correlation coefficient to assess the overall relationship in the whole region (Hou et al., 2021, Cord et al., 2017), and to duly represent the large spatial variation in both ESs and their potential influencing factors, we propose a new approach to investigate their relationship at a grid level for the assessment of synergies and tradeoffs.

2. Methods

2.1. Study area

Our study area involves four Nordic countries: Denmark, Finland, Norway, and Sweden (from 3°E to 32°E, from 54°N to 72°N). Norway is located in the western part of Scandinavia, in Northern Europe, and it is covered by forest and agriculture land by 37 % and 4 %, respectively (Zhou et al., 2021). Sweden, bordering Norway to the west, and Finland to the northeast, is the largest country among the four. Afforestation in Sweden began at the beginning of the 20th century, and it increased the ratio of forest until the 1960 s, but after that the ratio declined (Blanco et al., 2017). In 2018 it is covered by forest and agriculture land by 66 % and 9 %, respectively (Zhou et al., 2021). In Finland, forest and agriculture cover about 71 % and 8 % of the country. In these three countries, the majority of forests are under intensive management (Ceccherini et al., 2020). In Denmark, agriculture plays an essential role (Vogdrup-Schmidt et al., 2019), and the country is covered by agriculture land by 73 % (Zhou et al., 2021).

2.2. Data

Based on data availability, 2003 and 2018 are selected as the initial and final year of our study period. A large amount of data has been used to estimate ESs, such as digital elevation model (DEM), land cover maps, PR, TE, watershed, reference evapotranspiration, soil texture, wood harvest volumes, and crop yields (Table 1). All raster data are resampled at the same spatial resolution (1 km grid).

2.3. Land cover dataset modification

The land cover dataset plays a central role for the quantification of many ESs (Sharp et al., 2014), but existing products have limitations in terms of accuracy and representation of key features (Bayer et al., 2021). Forest is the dominant land cover in the Nordic region, and it is under intensive management (Ceccherini et al., 2020, Schelhaas et al., 2018). However, forest harvest goes largely undetected by land use products, thereby potentially ignoring the effect of forest management on ESs (Zhou et al., 2021). Satellite-derived data of changes in forest cover (losses and gains) are more accurate and available at high resolution (30 m), and they proved to offer valuable opportunities to map harvest events as they can capture interannual disturbances (Ceccherini et al., 2020). However, they lack the classification of non-forest land cover classes, thereby limiting their application in studies assessing all types of land cover. In order to retain the high accuracy on forest harvest areas and the spatial extension of multiple-class land cover products, we elaborated an advanced land cover dataset for the Nordic region where the land cover dataset from European Space Agency's Climate Change Initiative (ESACCI) (ESA, 2017), the global forest change (GFC) maps (Hansen et al., 2013), and the forest harvest maps (Ceccherini et al., 2020) are consistently integrated into one product. Each of these datasets has been individually used in recent years (Huang et al., 2020, Ceccherini et al., 2020, Hu et al., 2021b, Hu et al., 2021a). The ESACCI land cover product provides annual global maps from 1992 to 2018 with high spatial resolution (300 m at the equator). These maps have high consistency in space and time. The forest harvest dataset from Ceccherini et al. (2020) provide annual maps of clear-cut forest harvest areas in European countries by detecting changes in forest cover from global forest change maps using Google Earth Engine platform (Gorelick et al., 2017). This forest harvest product is produced from the GFC maps and is available at high spatial resolution (30 m) from 2001 to 2018.

Table 1
Data used in the analysis and source. USGS: United States Geological Survey, NASA: The National Aeronautics and Space Administration, FAO: The Food and Agriculture Organization of the United Nations, GLOBIO: Global biodiversity model for policy support, ESDAC: European Soil Data Centre.

Data	Source	website
Boundary for Nordic countries	DIVA-GIS	https://www.diva-gis.org/gdata
Land cover	ESACCI	https://www.esa-landcover-cci.org/
Forest change	Global forest change	https://earthenginepartners.appspot.com/science-2013-global-forest
Temperature	Climate Data Store - Copernicus	https://cds.climate.copernicus.eu/cdsapp#!/dataset/reanalysis-era5-land-monthly-means?tab=overview
Digital elevation model	USGS	https://www.usgs.gov/coastal-changes-and-impacts/gmted2010
Watershed	HydroBASINS	https://www.hydrosheds.org
Reference Evapotranspiration	CGIAR Platform for Big Data in Agriculture	https://figshare.com/articles/dataset/Global_Aridity_Index_and_Potential_Evapotranspiration_ET0_Climate_Database_v2/7504448/3
Net Primary productivity	MOD17A3H products	https://lpdaac.usgs.gov/products/mod17a3hv006/
Soil texture	Global Soil Assimilation Database, FAO	https://www.fao.org/soils-portal/data-hub/soil-maps-and-databases/harmonized-world-soil-database-v12/en/
Population	NASA	https://sedac.ciesin.columbia.edu/data/collection/gpw-v4
Road network	GLOBIO	https://www.globio.info/download-grip-dataset
Annual roundwood product statistics for Nordic countries	FAO	https://www.fao.org/faostat/en/#data
Annual crop product statistics for Nordic countries	FAO	https://www.fao.org/faostat/en/#data
Rainfall erosivity	ESDAC	https://esdac.jrc.ec.europa.eu/themes/rainfall-erosivity-europe
Precipitation	ClimateDT	https://www.ibbr.cnr.it//climate-dt/?action=help&id=ratio
Livestock	Research Article	https://journals.plos.org/plosone/article?id=https://doi.org/10.1371/journal.pone.0217166

We design a set of systematic procedures to update the land cover maps of the ESACCI dataset for 2018 and 2003 to include forest harvest events as follows. For modifying land cover map in 2018, we calculate the accumulated forest harvest ratio in each grid from 2004 to 2018 and integrate the threshold given in walking table for aggregating land covers (ESA, 2017). If the harvest ratio in a grid is higher than or equal to 85 %, we convert this grid to sparse vegetation. If the ratio is higher than or equal to 50 % but lower than 85 %, we convert the grid to mosaic cover. If the ratio is higher than or equal to 15 %, but lower than 50 %, the grid is converted to mosaic trees. Otherwise, the grid does not change. These three classes, sparse vegetation, mosaic cover and mosaic trees, are coded differently to distinguish with the classes in original ESACCI land cover dataset, which does not include the harvested forest class (hence our needs to define proxies). Furthermore, if a grid does not experience harvest and it is not classified as forest in the ESACCI, but the corresponding grid in the global forest change map has more than 50 % forest cover in 2018, we convert the land cover classes in the ESACCI to forest. To assign the type of forest (coniferous or deciduous), we use a random sample method based on the relative abundance of forest types in the ESACCI land cover map in 2018. We also modify land cover maps in 2003. If a grid in 2018 is classified as harvested, then this grid is classified as forest in 2003, again with a random sample method based on the relative abundance of forest types to identify it as coniferous or deciduous. As in 2018, if a grid does not experience harvest and it is not classified as forest in the land cover map in 2003, but the corresponding grid in global forest change map has more than 50 % forest cover in 2003, we convert the land cover class to forest with the random sample method.

2.4. Ecosystem services evaluation

We focused on six ESs (i.e., HQ, SR, WY, CS, CP, and WP) based on their crucial roles in Nordic countries. HQ, WY, and SR are modelled by applying the model INVEST (Integrated Valuation of Ecosystem Services and Tradeoffs) v3.9.0 (Posner et al., 2016) to the advanced land cover dataset at a spatial resolution of 1 km. INVEST provides a set of effective tools for evaluating ESs and it is designed to support policy makers for nature resources management (Sharp et al., 2014). It produces spatially explicit results and has been used for a variety of purposes, such as exploring the potential impact to biodiversity (with HQ as a proxy) from land cover changes and other threat factors (Sallustio et al., 2017, Hou et al., 2021), or changes in SR and WY due to climate change (Bouguerra and Jebari, 2017, Feng et al., 2020, Hamel et al., 2015).

The other ESs are estimated by combining specific datasets. For CS, we use the net primary productivity (NPP), and for CP and WP national statistics with the FAO (The Food and Agriculture Organization of the United Nations) data are used (FAO, 2020). These statistics are projected at a grid level according to the area of cropland from ESACCI and forest harvest maps (Ceccherini et al., 2020), respectively.

2.4.1. Habitat quality (HQ)

Biodiversity faces increasing threats from climate change and anthropogenic activities (Harfoot et al., 2021, Leclère et al., 2020). INVEST considers biodiversity as an attribute of nature systems and uses HQ as a proxy (Sharp et al., 2014). HQ refers to ecosystem's ability for providing resources for survival, reproduction and population persistence (Hall et al., 1997). In each grid x, the habitat quality $HQ(x)$ is calculated as,

$$HQ(x) = S(x)\cdot\left(1-\left(\frac{t(x)^z}{t(x)^z+k^z}\right)\right) \quad (1)$$

where S is the habitat suitability, t is the threat level and z and k are scaling parameters. Computing HQ requires information on land cover classes and relevant parameters to assess the threats. In general, we refer to previous studies, such as Sallustio et al. (2017), Sharp et al. (2014), Larson et al. (2004) and Di Febbraro et al. (2018) for more details. In this study, we use the advanced ESACCI land cover dataset so to capture the threats to HQ from forest harvest activities. This is modelled as a change in land cover, from forest to sparse vegetation or mosaic landscape, as each land cover type has a specific value in terms of habitat suitability (Sallustio et al., 2017). To consider the forest harvest effect, the habitat suitability of newly introduced sparse vegetation, mosaic cover and mosaic trees in the advanced ESACCI are set to 70 % of the corresponding values of habitat suitability in the original ESACCI land cover dataset (Larson et al., 2004). Proximity to urban, road and cropland are threat factors and the functions governing the decay of the threat at increasing distances are exponential, linear, and linear for these factors, respectively. The road network is from the Global Roads Inventory Project for Europe (Meijer et al., 2018). Cropland and urban is from the advanced ESACCI land cover dataset (ESA, 2017).

2.4.2. Water yield (WY)

INVEST is used to assess WY, according to the Budyko curve and annual mean precipitation (Sharp et al., 2014). The annual WY in each grid x, $WY(x)$, is calculated as,

$$WY(x) = P(x)\cdot\left(1 - \frac{AET(x)}{P(x)}\right) \tag{2}$$

where $P(x)$ is the annual mean precipitation, $AET(x)$ is the annual actual evapotranspiration. $AET(x)/P(x)$ is the evapotranspiration portion of water balance of each land cover in grid x and can be obtained from the Budyko curve (Zhang et al., 2004). The annual mean precipitation $P(x)$ is obtained from ClimateDT (Marchi, 2021), a scale free web-GIS system able to provide climatic variables at global scale data using a dynamic downscaling approach (Marchi et al., 2020), at 1 km spatial resolution. We use the 5-year mean with centers in 2003 and 2018 to avoid the impact of the fluctuation of the climate variables. The maximum root burial depth of soil and plant available water content are from the European Soil Database version 2.0 (Panagos, 2006), released by European Soil Data Centre (ESDAC). The land cover dataset is from the advanced ESACCI with the above-mentioned modification. Watershed is based on the HydroBASINS database. These parameters are needed to calculate $AET(x)$. The evaporation factor for each land cover class is needed to calculate $AET(x)$, and it is based on previous studies, such as Lehner and Grill (2013) and Hou et al. (2021). More specific information for computing WY can be found in Sharp et al. (2014).

2.4.3. Sediment retention (SR)

We compute SR with the following model:

$$SR(x) = R(x)\cdot K(x)\cdot LS(x)\cdot(1 - C(x)\cdot P(x))\cdot SDR_i \tag{3}$$

in each grid x, and R, K, LS, C and P are rainfall erosivity, soil erodibility, slop length-gradient factor, crop-management factor, and support practice factor, respectively. SDR is the sediment delivery ratio which can be computed from the upslope area and downslope flow path (Sharp et al., 2014). In INVEST, the SDR model adopts the parameterization proposed by Borselli et al. (2008), which is relatively simple and spatially explicit. With Equation (3), the index of SR is the avoided soil loss due to the land cover compared to bare soil (Sharp et al., 2014). The R parameter is from the rainfall erosivity in Europe (Panagos et al., 2015), released by ESDAC. The K parameter is calculated using the erosion-productivity impact calculator (Sharpley, 1990) using the Harmonized World Soil Database (Nachtergaele et al., 2010) v1.2 released by Food and Agriculture Organization of Unite Nation (FAO). The digital elevation model is from the Global Multi-resolution Terrain Elevation Data provided by U.S. Geological Survey (USGS) (Danielson and Gesch, 2011). The modified land cover dataset from ESACCI and watershed from HydroBASINS database are also needed. More information about the method is available in Sharp et al. (2014).

2.4.4. Carbon sequestration (CS)

The net primary productivity (NPP) was used as a proxy for evaluating CS. In each grid x, the relationship between CS and NPP is

$$CS(x) = 1.63\cdot NPP(x) \tag{4}$$

as the vegetation captures on average 1.63 units of carbon per unit of NPP (Li and Zhou, 2016, Hua et al., 2021). The annual NPP dataset is from Moderate Resolution Imaging Spectroradiometer (MODIS) MOD17A3HGF version 6. We use 5-year averages centered in 2003 and 2018 to present the NPPs in 2003 and 2018 to avoid potential bias and errors in single-year data.

2.4.5. Crop production (CP)

Crop production is closely related to the agriculture land in Nordic countries, identified with the land cover dataset from ESACCI. The original land cover classification is aggregated into the IPCC generic classes using the walking table given in ESA (2017). The crop production dataset includes the main crops in the four Nordic countries according to FAOSTAT (FAO, 2020). These main crops are cereals, oil-crops, vegetables, among others. We then spatialize the crop production statistics in each country j to each grid (denoted as $CP_j(x)$), according to area share of the agriculture land,

$$CP_j(x) = \frac{Area_{AGR,j}(x)}{\sum_i Area_{AGR,j}(x)}\cdot\sum_k Crops_j \tag{5}$$

where $Area_{AGR,j}(x)$ is the area of agriculture land in grid x in country j, $\sum_i Area_{AGR,j}(x)$ is the sum of all the grids classified as agriculture in country j, and $\sum_k Crops_j$ is the sum of all the crop products in country j. For the national statistics and land cover dataset, we use the 5-year mean with centers in 2003 and 2018 to avoid the impact of annual fluctuations.

2.4.6. Wood product (WP)

Roundwood production is from forest harvest, a key asset of the economies in Nordic countries. Zhou et al. (2021) mapped forest harvest areas in Nordic countries following the methodology provided by Ceccherini et al. (2020). We adopt the same approach to obtain the forest harvest maps in Nordic countries. The national statistics for roundwood of the four Nordic countries is from FAOSTAT (FAO, 2020). We then spatialize the roundwood statistics to each grid (denoted as $WP(x)$), according to the share of the harvested area in each country j,

$$WP_j(x) = \frac{Area_{FH,j}(x)}{\sum_i Area_{FH,j}(x)}\cdot\sum_k RoundWood_j \tag{6}$$

where $Area_{FH}$ is the harvested area in the grid, $\sum_i Area_{FHj}(x)$ is the total harvested area in each country j, and $\sum_k RoundWood_j$ is the sum of all the roundwood products in country j. For the national statistics, land cover dataset and annual harvest ratio, we use the 5-year sum with centers in 2003 and 2018 to reduce the impact of annual fluctuations.

2.5. Potential influencing factors and their relationship with ecosystem services

The most relevant potential influencing factors in the Nordic regions that are considered in our analysis are TE, PR, PD, LS, EL, and changes in land cover, especially, those involving AGR and FOR. The sources of these datasets are given in Table 1. For TE and PR, we use the 5-year mean with centers in 2003 and 2018 to avoid the impact of fluctuations in climate variables. For LS, data are only available for Norway at a municipality level from 1949 to 2015 at irregular time intervals. The linear interpolation/extrapolation method is used to obtain the data in 2003 and 2018. We investigate the correlation between ESs and the potential influencing factors using the Spearman's correlation coefficient (denoted as ρ) in 2003 and 2018.

Due to large spatial variability of ESs and influencing factors, the pairwise relationship is investigated in each grid cell. We first calculate the changes of individual ESs (denoted as ΔES) between 2018 and 2003, and the changes of the influencing factors (denoted as ΔIF). We then classify ΔES and ΔIF (generically denoted as ΔVar) into five levels with chosen thresholds in every grid x (denoted as ΔVar_c),

$$\Delta Var_c(x) = \begin{cases} -1, & \Delta Var(x) \leqslant -t_2 \\ -0.5, & -t_2 < \Delta Var(x) \leqslant -t_1 \\ 0, & -t_1 < \Delta Var(x) < t_1 \\ 0.5, & t_1 < \Delta Var(x) \leqslant t_2 \\ 1, & \Delta Var(x) \geqslant t_2 \end{cases} \tag{7}$$

where t_1 and t_2 are chosen thresholds. In general, t_1 is a very small value and t_2 is chosen according to the histogram or percentile of the variable. In our paper, we use $t_1 = 0.005$ and t_2 is a value around 95 % percentile of each ΔVar. With this approach, the values 1 and −1 can be interpreted as strong positive or strong negative change from 2003 to 2018, respectively, and the values 0.5 and −0.5 can be interpreted as medium positive and medium negative change, respectively. The value 0 can be interpreted as no change. For changes in land cover, such as FOR and AGR, the changes only have three states, 1, 0, and −1 to indicate increase, no change, and decrease of that land cover type, respectively.

With this approach, we can then further investigate the relationship between each combination of influencing factor and ES,

$$\varsigma(x) = \Delta ES_c(x) \cdot \Delta IF_c(x) = \begin{cases} 1, & \text{strong positive} \\ 0.5, & \text{medium positive} \\ 0.25, & \text{weak positive} \\ 0, & \text{independent} \\ -0.25, & \text{weak negative} \\ -0.5, & \text{medium negative} \\ -1, & \text{strong negative} \end{cases} \quad (8)$$

where if $\varsigma = 1$ there is a strong positive relationship between the change in the influencing factor and ES, and if $\varsigma = -1$ there is a strong negative relationship. When $\varsigma = 0$, the change of the influencing factor and the change of ES are independent. Other relationships are defined in Eq. (8).

2.6. Relationships between ecosystem services

In addition to the relationship between ESs and influencing factors, we also assess the potential relationship between ESs. Due to the non-normality nature of ESs and in line with previous studies (Yue et al., 2022), we use the Spearman rank correlation to investigate pairwise relationship between each pair of ESs (Cord et al., 2017). Positive or negative correlations indicate an overall synergy or a tradeoff in the relationship in the whole region.

Furthermore, the pairwise relationship between ESs is investigated in each grid cell, similarly to the previous section. We first calculate the changes of individual ESs (denoted as ΔES) between 2018 and 2003. We use Eq. (7) to classify ΔES into five levels, and then investigate the pair-wised relationship between ESs in terms of synergies and tradeoffs using the following equation,

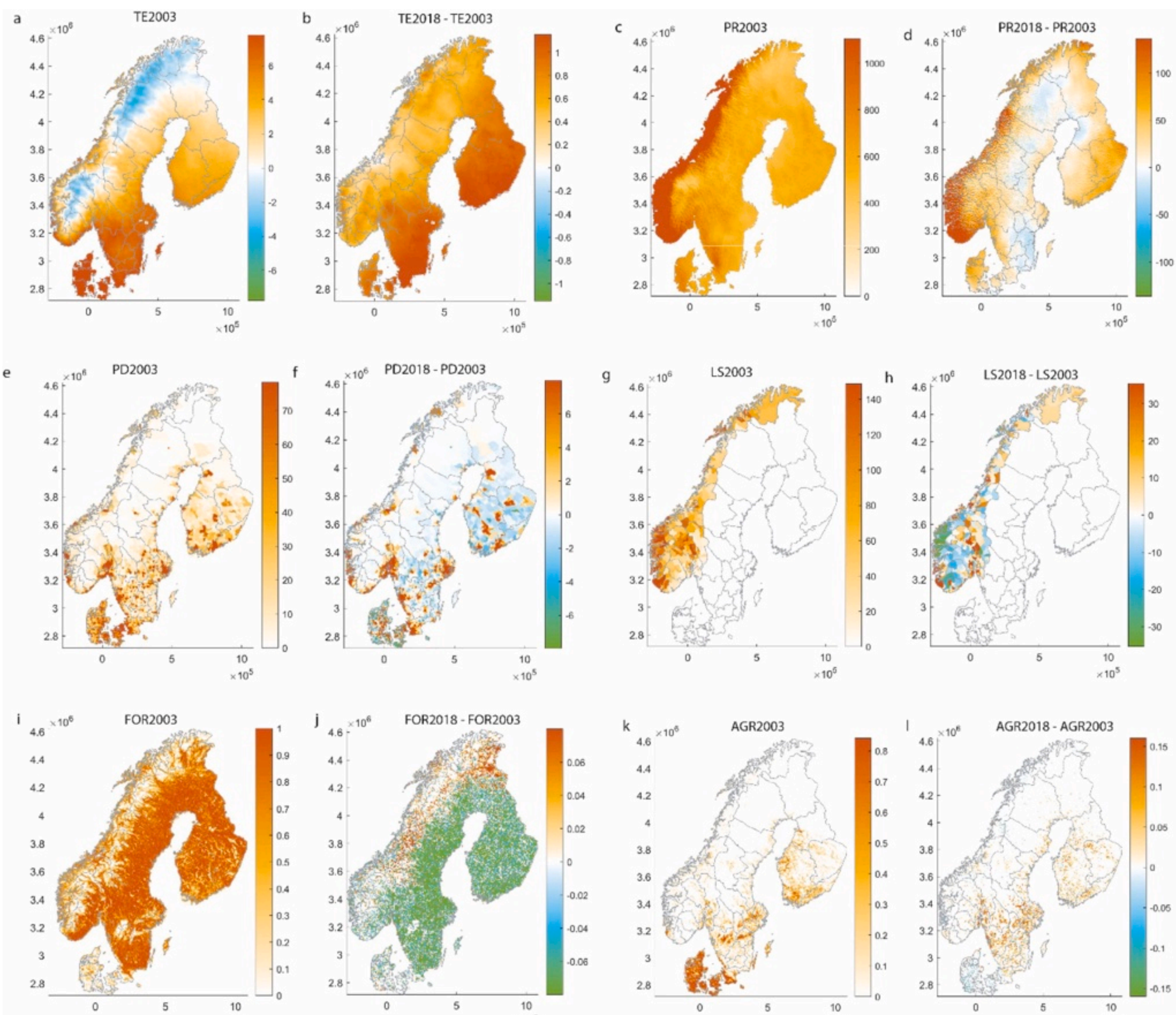

Fig. 1. States of climate, land covers, and livestock in 2003 and changes between 2018 and 2003 in Nordic countries. TE: temperature, PR: precipitation, PD: population density, LS: livestock, FOR: forest, AGR: agriculture. The maps are aggregated to 5 km for visualization purposes only. The scales of color bars are different in each subfigure. Units: a and b in °C, c and d in mm, e and f in person/km^2, g and h in kg/km^2, i-l in fraction of a grid.

$$\xi(x) = \Delta ES_{c,1}(x) \cdot \Delta ES_{c,2}(x) = \begin{cases} 1, & \text{strong synergy} \\ 0.5, & \text{medium synergy} \\ 0.25, & \text{weak synergy} \\ 0, & \text{independent} \\ -0.25, & \text{weak tradeoff} \\ -0.5, & \text{medium tradeoff} \\ -1, & \text{strong tradeoff} \end{cases} \tag{9}$$

Positive values of ξ indicate that there is a synergy relationship between the changes of the two ESs. This synergy is strong when $\xi = 1$. Similarly, negative values of ξ indicates that there is a tradeoff relationship between the changes of the two ESs, and $\xi =$ -1 indicates that there is a strong tradeoff. When $\xi = 0$, the changes of the two ESs are independent. Other relationships are defined in Eq. (9). This method is based on the fundamental understanding of the changes of ESs. If both paired ESs are increased during the same period, they show a synergy relationship, and if their changes are with opposite direction, they show a tradeoff relationship. Furthermore, by considering the intensity of the changes, we can quantify the degree of these relationships via Eq. (9).

3. Results

3.1. Changes in influencing factors and ecosystem services

During the study period, the climate, land covers, and LS have changed in Nordic countries (Fig. 1). The effect of global warming is evident, especially in southern Sweden and Finland, with average temperature increase of 0.7 °C in the study region (Fig. 1b). Precipitation is more intensive along the coastline of Norway (Fig. 1c), where it has also dramatically increased. However, it has decreased at high latitude and in the southern part of Sweden (Fig. 1d). In all the domain, the average increase in precipitation is 37 mm. In Nordic countries, population is primarily concentrated around the main cities, and from 2003 to 2018 PD has increased along the coast in Norway and Sweden, with declines in rural areas in Sweden and Finland. The average change in PD is an increase by 2 persons per km^2 in the study region. Livestock data are only available for Norway, and their changes do not show a clear pattern. Grazing pressure from LS has generally decreased in the west

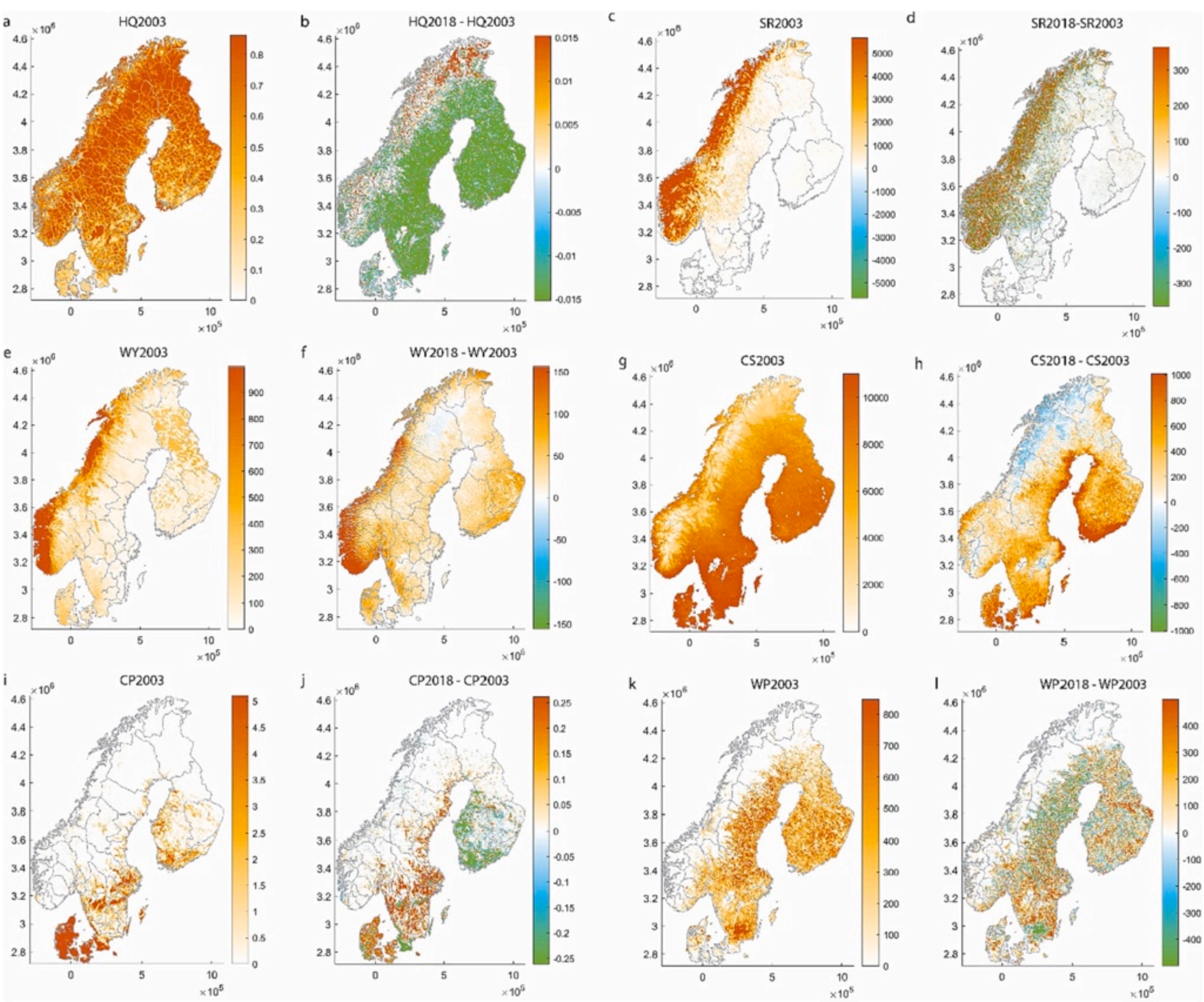

Fig. 2. Ecosystem services in 2003 and the changes between 2018 and 2003. The maps are aggregated to 5 km for visualization purposes only. The scales of color bars are different in each subfigure. Units: a and b have no unit, c and d in t/ha yr^{-1}, e and f in mm, g and h in kg. C/m^2, i and j in M t, WP in m^3. HQ: habitat quality, SE: soil erosion, WY: water yield, CS: carbon sequestration, CP: crop product. WP: wood product.

and south-west part of the country, while it has increased at high latitude and in the central mountainous areas, primarily as a consequence of global warming that favored vegetation expansion (Speed et al., 2019) (Fig. 1g-h). Changes in forest areas include both temporary disturbances from forest management and expansion of agricultural land (smaller fraction). Forest management is highly intensive in Sweden, Finland, and southeast Norway, while forest areas have expanded at high latitudes (Fig. 1i-j). Annual (average 2001–2005) forest harvest areas in the three countries were around 13.2 Mha in Sweden, 10.6 Mha in Finland, and 1.8 Mha in Norway. In 2018 (average 2016–2020) they were around 22.1 Mha in Sweden, 19.6 Mha in Finland, and 4.3 Mha in Norway. AGR has deceased in Denmark (–33.7 kha), but it has increased in Sweden (446.7 kha), Finland (196.1 kha), and Norway (99.9 kha) (Fig. 1k-l).

The states of ESs in 2003 and their changes between 2018 and 2003 are shown in Fig. 2, with the corresponding statistics in Table 2. In general, the HQ is decreased and there is 21.3 % of the grids with HQ degradation and only 2.6 % of the grids where HQ is increased. Spatial distribution shows that HQ is decreased in most areas of Sweden and Finland, but it is increased at high latitude and in the mountainous region in Norway (Fig. 2b). This might be due to greening because of global warming (Zhu et al., 2016). SR has increased in Norway, mostly connected to increased precipitation. SR decreased in some regions in Sweden and Finland (Fig. 2d and Table 2), mostly connected to decreased precipitation (Fig. 1d). There are no visible changes of SR in Denmark, mainly due to that precipitation in this region is increased (Fig. 1d) while agriculture activity is decreased (Fig. 1i), with the two effects compensating for each other. There is 40.7 % of the grids with increased SR, and 41.4 % where the SR have decreased. WY increased almost in the whole region, except in the northern Sweden (Fig. 2f), and the spatial pattern is like the one of change in PR (Fig. 1d). On average, the WY is increased by 44 mm, and up to 75.2 % of the grids have increased and 19.4 % decreased. CS is based on annual mean NPP, which has increased in most of the areas (75 % of the grids) during the study period because of warmer conditions and extension of the growing season (Fig. 2h). There are also places where NPP has decreased (25 % of the grids), especially at high latitudes. These areas experienced increases in both temperature and precipitation. A similar trend is also observed by other studies in the same or other boreal regions (Ding et al., 2020, Winkler et al., 2021), and can be connected to an emerging browning trend associated with declines in leaf area index. Reasons are still unclear, but climate changes as increasing atmospheric CO_2 concentrations and increased summer cloud cover can trigger a negative response in boreal tundra. A study found that Eurasian tundra shows a positive greening trend for the years 1982–2017 but a reversal in trend sign (e.g., browning) for the years 2000–2017 (Winkler et al., 2021), which is similar to the time period used in our analysis. Total crop production in the four countries has changed from 14.4 Mt to 14.6 Mt in Denmark, 5.9 Mt to 4.9 Mt in Finland, 1.9 Mt to 1.8 Mt in Norway and 9.3 Mt to 9.0 Mt in Sweden. The crop total production is thus increased in Denmark, but decreased in Finland, Norway, and Sweden. On the grid level, CP is increased in southeast part of Norway and Sweden but decreased in Finland and southernmost part of Sweden (Fig. 2j). In Sweden and Norway, the land cover dataset shows an expansion of agriculture land (Zhou et al., 2021), even though annual statistics from FAO showed an opposite trend in agricultural area (FAO, 2020). CP is increased in Denmark despite agriculture land has decreased (Fig. 1l), and this is mainly due to intensification and increases in crop yields (FAO, 2020). In general, expansion of global trade of food products and commodities, and progressive migration from rural to urban areas also influence the trends in agricultural production.

The 5-year sum of roundwood production centered in 2003 and 2018 in all four countries is increased, from 12 Mm^3 to 19 Mm^3 in Denmark, from 266 Mm^3 to 317 Mm^3 in Finland, from 44 Mm^3 to 61 Mm^3 in Norway and from 362 Mm^3 to 373 Mm^3 in Sweden. The spatial distribution of the changes in WP is shown in Fig. 2l. Obviously, harvested sites differ from the two time periods, but forest management in the countries occurs in relatively small plots at a sub-grid level, so that intensity areas can be appreciated. WPs are primarily sourced from southeast Norway, and largely widespread in Sweden and Finland. In the latest years, WPs from Southern Sweden have generally increased.

3.2. Ecosystem services and potential influencing factors

The overall static correlation (i.e., for 2003 and 2018 independently) for the most relevant combinations of potential influencing factors and ESs are shown in Table 3. PR is slightly negatively correlated with HQ in both 2003 and 2018, and positively correlated with SR (as more rainfall increased the R factor in Equation (3)) and especially WY (as PR is clearly the main driver of WY). No significant correlation is found with CS and CP. TE is negatively correlated with HQ, SR, and WY. The negative correlation with WY occurs despite this ES has increased in most of the domain, but high temperature induces high evapotranspiration. TE is highly positively correlated with CS, as higher temperature drives higher NPP in areas where vegetation activity is primarily constrained by low temperature. For the same reason, TE is also positively correlated with CP. PD is negatively with HQ, since proximity to population introduces more threats to HQ. The correlations between LS and the ESs are generally low (Table 3). No major differences are found in

Table 2
Statistics of the changes in ecosystem services (ΔES) and influencing factors from 2003 to 2018 in Nordic countries. TE: temperature, PR: precipitation, PD: population density, LS: livestock, HQ: habitat quality, SE: soil erosion, WY: water yield, CS: carbon sequestration, CP: crop product. WP: wood product.

	mean	5th percentile	95th percentile	Positive grids	Negative grids
ΔTE (°C)	0.72	0.32	1.15	99.9 %	0.1 %
ΔPR (mm)	37	–33	153	75.5 %	24.5 %
ΔPD (person/ km^2)	2.38	−1.89	6.90	30.3 %	67.1 %
ΔLS ((kg/ km^2)	3.72	−24.8	35.4	56.2 %	43.8 %
ΔHQ	−0.017	−0.14	0	2.6 %	21.3 %
ΔSR (t yr^{-1})	8.46	−2.73	2.84	40.7 %	41.4 %
ΔWY (mm)	43.8	−18.8	186	75.2 %	19.4 %
ΔCS (kg. C/ m^2)	313	−331	1163	75.0 %	24.9 %
ΔCP (M t)	0.03	−0.25	0.26	6.9 %	10.3 %
ΔWP (m^3)	31.1	−1034	1256	28.4 %	21.4 %

Table 3
Spearman's correlation of the ecosystem services and potential influence factors. WP is not considered because it is due to human activity (forest harvest of specific sites) and it is independent from these influencing factors in the time frame of our analysis. PR: precipitation, TE: temperature, PD: population density, LS: livestock: HQ: habitat quality, SR: sediment retention, WY: water yield, CS: carbon sequestration, CP: crop product. All the correlation coefficients ρ in the table are significant at 0.05 level.

	Spearman's Correlation ρ (2003)	Spearman's Correlation ρ (2018)
PR/HQ	−0.11	−0.11
PR/SR	0.32	0.36
PR/WY	0.62	0.67
PR/CS	0.07	0.04
PR/CP	0.03	0.02
TE/HQ	−0.29	−0.33
TE/SR	−0.25	−0.27
TE/WY	−0.25	−0.19
TE/CS	0.90	0.91
TE/CP	0.42	0.44
PD/HQ	−0.36	−0.38
LS/HQ	−0.02	−0.02
LS/SR	0.08	0.04
LS/CP	0.06	0.07

the type of correlation between influencing factors and ES between 2003 and 2018.

The spatial distribution of the relationship between ESs and the potential influencing factors is shown in Fig. 3, and the shares of the grids with these relationships classified as strong positive, medium positive, weak positive, weak negative, medium negative, and strong negative are shown in Table 4. In this table, only the grids with changes (i.e., non-zero values) are considered when calculating the percentages.

For PR and HQ, there are 76 % of grids showing a negative relationship, and the majority is weak negative (63 %). SR, WY, and CS show positive relationship with PR in most grids (54.8 %, 96 %, and 72 %, respectively), and the majority is weak positive. The positive relationship between PR and SR mostly take place in Norway (Fig. 3a). PR and CS are positively correlated in southern Norway, Finland, and Denmark, whereas there is a negative relationship at high latitudes and in south-eastern Sweden (Fig. 3b). The relationship between TE and HQ is negative in most grids (87 %), with 54 % showing medium negative (Fig. 3c). A positive relationship is found at high latitudes, where higher temperature can favor vegetation growth and improve habitat quality. TE shows predominantly positive relationships with WY, and CS, mainly due to increasing TE in all grids, as WY, and CS are also increased during the study period (Fig. 3d, Table 4). SR does not show clear relationship with TE at a grid level (Table 4), even though the overall correlation coefficient is negative (Table 3). In general, since TE is increased in all grids, the spatial pattern mainly follows the pattern of the ESs. PD and HQ show positive relationship in two thirds of the grids, which is mostly an artefact as HQ and PD has decreased in many areas (Fig. 1e, Fig. 2a, and Fig. 3e). LS does not show clear pattern of changes (Fig. 1h), so does the relationship between LS and HQ, SR, CS and CP. The only exception is at high latitudes and in southwestern Norway, where negative values for LS-CS dominate (Fig. 3f). FOR and HQ have positive relationship in many grids (72 %, Fig. 3g) since both decreased during the study period (Fig. 1g and Fig. 2a). This decline in forest cover includes the temporary disturbances of forest management, which contributes to declines in HQ. On the other hand, FOR has negative relationship with CS in most of the grids (80 %). This means that a decline in forest cover usually co-occur with an increase in carbon sequestration. The latter can be explained by the fact that forest harvest replaces mature forest where carbon sequestration rates are low with new trees, which have higher growth rates (and hence higher NPP values). The spatial patterns of the relationship between FOR and CS are shown in Fig. 3h, from which we can see that the negative relationship largely overlaps with the forest harvest sites. At a Nordic level, the majority of the grids shows a positive relationship between AGR and HQ, primarily driven by AGR contraction in Denmark (Fig. 3i). Where agriculture is expanding, there is a negative relationship as it is one of the main threats to HQ (which declines). There is no clear relationship between SR and AGR and FOR, since SR is driven by precipitation and changes in land cover and land management (Table 4 and Fig. 3j).

3.3. Relationships between ecosystem services

We first study the overall correlation of each pair of ESs (Table 5) using the Spearman's correlation coefficient to identify synergies or tradeoffs. In general, many correlation coefficients are low due to the large spatial variation in each ES (Fig. 2). There are 10 pairs of ESs which have tradeoff relationships ($\rho < 0$), and 5 pairs of ESs with synergy relationships ($\rho > 0$), and these relationships are consistent in 2003 and 2018. HQ is negatively correlated with WY, CP, and WP. In other words, higher WY, CP, and WP are usually associated with lower HQ. HQ is also negatively correlated with CS, mostly because in Nordic countries higher CS usually follows forest harvest (as young trees have higher growing rates than mature trees), which is a driver of declines in HQ. SR shows a synergy with WY, since stronger and intense precipitation leads to higher R factor (Equation (3)) and more precipitation contributed to higher WY, and a tradeoff with CS (as increased vegetation activity

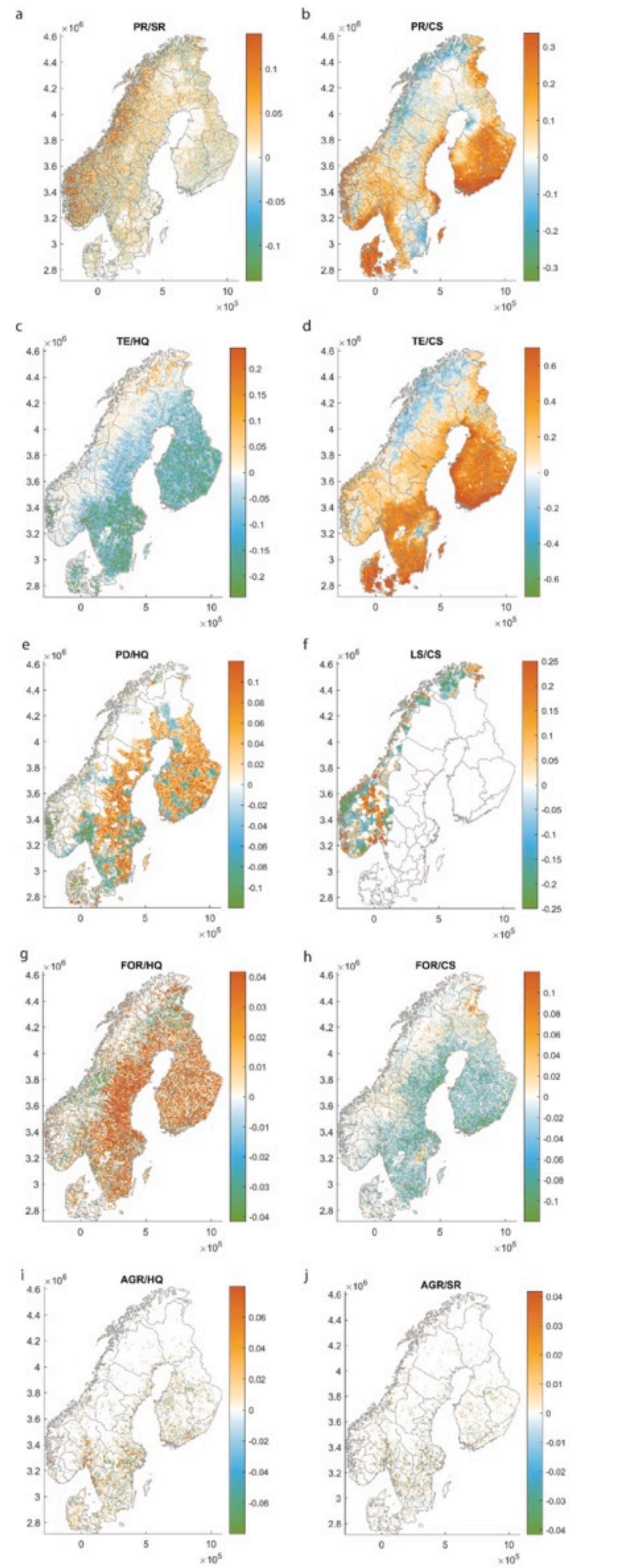

Fig. 3. Spatial relationship between the potential influencing factors and ESs. Values (obtained from Eq. (8)) indicate the relationship between the change in the influencing factor and ES in grid level. PR: precipitation, TE: temperature, PD: population density, LS: livestock: HQ: habitat quality, SR: sediment retention, WY: water yield, CS: carbon sequestration, CP: crop product. FOR: forest, AGR: agriculture land. The maps are aggregated to 5 km for visualization purposes only. The scales of color bars are different in each subfigure.

Table 4
Relationship between ESs and potential influencing factors. Numbers are given in percentage of grids which are changed in the study area. PR: precipitation, TE: temperature, PD: population density, LS: livestock: HQ: habitat quality, SR: sediment retention, WY: water yield, CS: carbon sequestration, CP: crop product. FOR: forest, AGR: agriculture.

	Strong positive	Medium positive	Weak positive	Total positive	Weak negative	Medium negative	Strong negative	Total negative
PR/HQ	0.3	6.1	18.2	24.5	63.0	12.1	0.4	75.5
PR/SR	2.7	10.3	41.8	54.8	35.3	8.0	1.9	45.2
PR/WY	2.8	6.4	87.2	96.4	3.5	0.0	0.0	3.6
PR/CS	0.2	14.4	57.2	71.7	24.8	3.3	0.1	28.3
PR/CP	0.0	7.3	44.5	51.7	44.1	4.2	0.0	48.3
TE/HQ	0.7	7.3	5.3	13.3	25.4	53.8	7.5	86.7
TE/SR	0.4	25.0	25.1	49.5	25.7	24.5	0.4	50.5
TE/WY	0.2	45.8	44.0	90.1	8.4	1.4	0.0	9.9
TE/CS	8.2	40.1	31.5	79.8	15.8	4.3	0.1	20.2
TE/CP	8.4	29.6	6.3	44.3	6.5	48.0	1.2	55.7
PD/HQ	0.4	12.3	50.8	63.5	21.0	14.3	1.2	36.5
LS/HQ	0.2	16.0	36.9	53.1	35.8	10.5	0.6	46.9
LS/SR	0.8	19.0	30.3	50.1	30.2	18.9	0.8	49.9
LS/CS	0.1	4.1	39.8	44.1	52.0	3.6	0.4	55.9
FOR/HQ	21.3	50.3	–	71.6	–	26.6	1.8	28.4
FOR/SR	4.2	46.8	–	51.0	–	45.4	3.7	49.0
FOR/CS	1.2	18.5	–	19.7	–	68.7	11.7	80.3
AGR/HQ	13.0	49.8	–	62.8	–	9.9	27.3	37.2
AGR/SR	4.4	41.4	–	45.8	–	49.5	4.7	54.2

Table 5
Spearman's rank correlation of each pair of ESs in 2003 and 2018. The table also show the type of the relationship, either synergy (S) or tradeoff (T). HQ: habitat quality, SR: sediment retention, WY: water yield, CS: carbon sequestration, CP: crop product, WP: wood product. All the correlation coefficients ρ are significant at 0.05 level.

ES pairs		Spearman's Correlation ρ (2003)	Interaction (2003)	Spearman's Correlation ρ (2018)	Interaction (2018)
HQ	SR	0.02	S	0.05	S
HQ	WY	−0.06	T	−0.11	T
HQ	CS	−0.28	T	−0.33	T
HQ	CP	−0.33	T	−0.35	T
HQ	WP	−0.13	T	−0.21	T
SR	WY	0.34	S	0.38	S
SR	CS	−0.30	T	−0.32	T
SR	CP	−0.13	T	−0.17	T
SR	WP	−0.14	T	−0.17	T
WY	CS	−0.33	T	−0.26	T
WY	CP	−0.004	T	−0.006	T
WY	WP	−0.22	T	−0.20	T
CS	CP	0.37	S	0.40	S
CS	WP	0.42	S	0.50	S
CP	WP	0.08	S	0.11	S

probably increases the soil retention capacity). WY has a tradeoff with CS, since the decreasing trend of WY in the harvested sites (Fig. 2e) contrasts with the higher CS (Fig. 2g). This relationship is also valid for WY and WP. CS has a synergy with CP and WP, since high CP mainly occurs in Denmark and southern Sweden (Fig. 2i) where CS benefits from higher temperature and the CS-WP relationship has been discussed above.

The spatial distribution of the pairwise relationships of the changes in ESs is shown in Fig. 4, and the intensity of the synergy or tradeoff is shown in Table 6. In general, the relationships have large spatial variations. For instance, there is an evident tradeoff between HQ and CS (Fig. 4a), and HQ and WP (Fig. 4c), mostly connected to forest harvest. For HQ and WP, the number of grids with a medium to strong tradeoff is larger than 25 %. The relationship between HQ and CP has large spatial variation (Fig. 4b), mainly due to different drivers of changes in CP. The synergy relationship (up to 53.9 % of the grids) between SR and WY mainly appears in the region with increasing PR, since PR is the main driver for both higher SR and WY (Fig. 4d). The relationship between changes in SR and changes in WP does not have a clear spatial pattern (Fig. 4e), since the WP does not have a clear pattern of changes, as discussed above. The changes of WY and the changes of CS have synergy in most of the grids (64.2 %), and the spatial pattern mainly follows the pattern of CS since WY is increased in most region (Fig. 4f). CS and CP have different relationships in different regions (Fig, 4 g). In total, 47 % of the grids have a synergy relation, mainly in Denmark, and 53 % a tradeoff relationship, mainly in Finland. The relationship between these two ESs is mixed and generally weak in Sweden. Due to no clear pattern of WP, as discussed above, the relationship between WP and CS does not have a spatial pattern (Fig. 4h), and the number of grids with synergies and tradeoffs are similar. In terms of intensity of the relationship across the domain, the pairwise combination of ES with about 25 % of the grids with a medium or strong synergy are CS/WP. The ESs with the larger spatial distribution of tradeoffs are HQ/CS and HQ/WP.

3.4. Elevation and ecosystem services relationships

We further investigate how the ES relationships change with elevation (Table 7) using the Spearman's correlation coefficient. Only results for 2003 are shown, since those for 2018 are very similar, and some ESs are omitted because they do not show clear spatial patterns (following the analysis in Fig. 4). There is a consistent tradeoff relationship between HQ and WY at different elevation levels, with the tradeoff that increases with altitude. This might be connected to the greening in alpine ecosystems as a response to higher temperatures, which drives increased HQ (Fig. 2b), while less precipitation results in lower WY (Fig. 1d). HQ and CP also show a consistent tradeoff relationship across different elevation levels, but with a decreased trend, as cropland is mostly located at lower altitudes. When elevation is below 800 m, the relationships between HQ and CS and WP are a weak tradeoff, but when elevation is above 800 m the relationships turn into a synergy. This might be correlated to the relatively widespread increases in HQ from enhanced vegetation growth in mountainous areas. SR and WY show a consistent synergy relationship since both are influenced by precipitation. A consistent tradeoff relationship between WY and CS is detected at all elevation levels, and the tradeoff relationship increases with altitude (e.g., WY is higher in the coastal area of western Norway, where CS is low). High WY is mainly related to precipitation and low CS is mainly due to low NPP values. There is a relatively strong synergy relationship between WY and CP at elevation lower than 100 m, meaning higher WY is associated with higher supply of CP. At all elevation levels, CS and WP show a consistent synergy relationship, for the same reason discussion in Section 3.2.

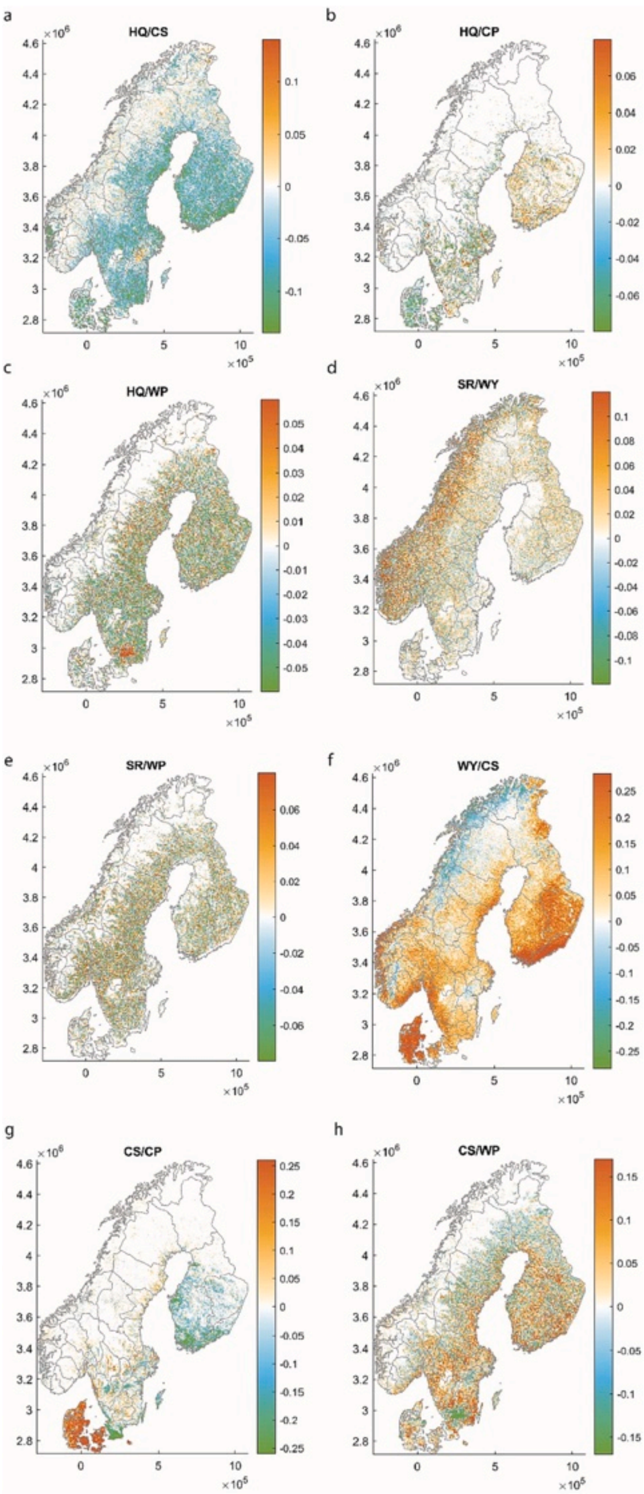

Fig. 4. Pairwise relationship of ESs. Positive and negative values (obtained from Eq. (9)) indicate a synergy or tradeoff relationship in each grid. PR: precipitation, TE: temperature, PD: population density, LS: livestock: HQ: habitat quality, SR: sediment retention, WY: water yield, CS: carbon sequestration, CP: crop product. FOR: forest, AGR: agriculture land. The maps are aggregated to 5 km for visualization purposes only. The scales of color bars are different in each subfigure.

4. Discussion

ES-related research is an active field with increasing contributions assessing ecosystem changes and their drivers in different regions (Mouchet et al., 2014, Cord et al., 2017). An analysis of ESs and associated changes in Nordic countries was missing, and this paper addresses this gap by assessing how multiple ESs changed over time and their potential influencing factors. Our study shows that ESs have changed during the study period, but the changes have large spatial variations resulting in low Spearman's correlation coefficients for most ESs pairs. When two ESs are driven by the same factors, the Spearman's correlation coefficient is high. For instance, WY and SR are both driven by PR and hence show a high positive correlation. Therefore, the interpretation of the correlation between ES and the influencing factors should be done with care, considering the spatial pattern of each individual element. A co-occurrence of a change (either positive or negative) does not automatically mean a direct causation, as well as pair of ESs that show synergies or tradeoffs are not necessarily correlated. Our analysis shows potential relationships and can help to identify expectations and directions of changes, and in some cases pointed out to specific mechanisms responsible of changes-response patterns. It also helps to understand the type of the pairwise relationships of ESs and offers a large-scale overview over the main trends in Nordic countries, with an overview of the main spatial differences and more evident relationships. After this large-scale screening, more specific interactions are to be followed up at a case-specific level, with supporting evidence of the relationship between the potential driver and ESs in the local context. This knowledge will ultimately support the design of management practices that can adapt influencing factors to secure ecosystem services.

In general, our study shows that supporting services (i.e., HQ) have a tradeoff relationship with regulating services (CS) or provisioning services (CP or WP). There is also a tradeoff between HQ and WY, which is opposite to other studies in other regions. For instance, Egoh et al. (2009) and Hou et al. (2021) found that HQ shows synergies with WY in South Africa and Tibetan Plateau, respectively. The use of the advanced land cover dataset shows that the tradeoff relationship with HQ is mainly due to forest management, as HQ primarily declines in the areas that are harvested. In areas not affected by forest management, such as at high latitudes in Norway and Sweden, HQ has a synergy relationship with regulating services, which is consistent with the other studies (Hou et al., 2021, Egoh et al., 2009). At the same time, forest management is highly correlated with CS, as it increases the carbon sink capacity of ecosystems. We acknowledge that the declines in HQ are not the result of direct measurements, but they are the outcomes of the INVEST model. Although the model has been parameterized with local specific conditions, the outcomes include uncertainties, and more research should investigate the accuracy at which it can represent the effects of forest management on HQ in boreal forests. HQ is also a generic indicator that is not species-specific, and different species may respond differently to the disturbances considered in our study (forest management, road, climate change, population). More specific analyses are required to identify options to reduce the potential adverse effects of forest management practices on HQ. Examples include selected tree harvest, continuous cover, or retention in the forest of varying proportions of deadwood materials.

We propose a new method for investigating the relationship of pairwise ESs at a grid level to assess synergies and tradeoffs. Our method is based on the dynamics of ESs and can further quantify the degree of the relationships. Li et al. (2017) have discussed another method for spatially explicit quantifications of the relationships among ESs, and their method is based on correlation analysis. The basic idea of our proposed method is similar, but in some sense more intuitive and it does not rely on the correlation analysis. Furthermore, we can quantify the degree of synergies and tradeoffs in each grid, as shown in Equation (9). Similarly, Qiu et al. (2018) adopt the pairwise correlation at different spatial scales, but at the grid scale they need to generate random samples

Table 6
Relationship for selected pairs of ESs. Numbers are given in percentage of grids which are changed in the study area. No change grids are excluded from the calculations. HQ: habitat quality, SE: sediment retention, WY: water yield, CS: carbon sequestration, CP: crop product, WP: roundwood product.

	Strong synergy	Medium synergy	Weak synergy	Total synergy	Weak tradeoff	Medium tradeoff	Strong tradeoff	Total tradeoff
HQ/SR	0.9	11.1	38.1	50.1	38.3	10.8	0.8	49.9
HQ/WY	0.0	3.0	7.2	10.2	75.4	14.0	0.4	89.8
HQ/CS	0.3	4.1	14.5	18.8	58.5	21.1	1.6	81.2
HQ/CP	0.6	9.9	38.2	48.6	31.7	15.1	4.6	51.4
HQ/WP	2.5	17.9	22.8	43.1	30.9	22.8	3.2	56.9
SR/WY	0.9	11.9	41.1	53.9	36.5	8.9	0.7	46.1
SR/CS	0.2	10.5	38.8	49.5	39.8	10.5	0.2	50.5
SR/CP	0.1	9.5	42.3	51.8	38.3	9.7	0.1	48.2
SR/WP	0.6	19.7	29.3	49.5	29.9	19.9	0.6	50.5
WY/CS	0.1	11.8	64.2	76.1	22.5	1.4	0.0	23.9
WY/CP	0.0	9.4	43.2	52.6	45.3	2.1	0.0	47.4
WY/WP	0.1	19.9	36.9	56.9	27.6	15.5	0.0	43.1
CS/CP	1.5	18.5	26.8	46.7	38.5	14.3	0.5	53.3
CS/WP	2.4	21.6	31.1	55.1	24.2	18.1	2.5	44.9

Table 7
Correlation for each pair of ESs. HQ: habitat quality, SE: sediment retention, WY: water yield, CS: carbon sequestration, CP: crop product, WP: roundwood product. EL: elevation. EL1: elevation lower than or equal to 100 m (coded as 1), EL2: elevation lower than or equal to 200 m but higher than 100 m (coded as 2), EL3: elevation lower than or equal to 400 m but higher than 200 m (coded as 3), EL4: elevation lower than or equal to 800 m but higher than 400 m (coded as 4), EL5: elevation higher than 800 m (coded as 5). The correlation coefficients significant at 0.05 level are indicated with *.

	EL1	EL2	EL3	EL4	EL5
HQ/WY	−0.22*	−0.06*	−0.11*	−0.10*	−0.43*
HQ/CS	−0.09*	−0.21*	−0.23*	−0.07*	0.51*
HQ/CP	−0.33*	−0.26*	−0.18*	−0.12*	−0.01*
HQ/WP	−0.01*	−0.12*	−0.14*	−0.08*	0.11*
SR/WY	0.21*	0.12*	0.19*	0.40*	0.20*
WY/CS	−0.06*	−0.11*	−0.05*	−0.28*	−0.43*
WY/CP	0.34*	0.02*	0.08*	0.08*	0.00
CS/CP	0.20*	0.16*	0.15*	0.03*	0.07*
CS/WP	0.06*	0.32*	0.40*	0.31*	0.21*

across the landscape, and the result will be a correlation coefficient. The method we propose results in maps of ESs relationships, and can be further used to investigate spatial patterns, as shown in Fig. 4.

Changes in land cover are among the main influencing factors for several ESs (Tolessa et al., 2017, Cabral et al., 2016), and their accurate representation is crucial to understand the changes in ESs and their relationships (Sharp et al., 2014). In this work, we created an advanced land cover dataset by combining the high-resolution land cover product from ESACCI with a forest database (GFC) to explicitly consider the influence of forest management. These two datasets have been widely verified and increasingly used in the literatures (Hu et al., 2021b, Ceccherini et al., 2020, Leirpoll et al., 2021, Li et al., 2018), but they have their own limitations. A full overview of their respective uncertainty is available in the original papers (Li et al., 2016, Li et al., 2018, ESA, 2017, Liu et al., 2018, Hua et al., 2018). One main limitation of the ESACCI land cover is the possible misclassification of land cover classes (Liang et al., 2019, Hua et al., 2018), which can influence our results. However, its accuracy has been quantified to be around 71 % at a global level, and cropland and forests are usually identified with higher accuracy (Pérez-Hoyos et al., 2017). The use of an advanced land cover dataset where we updated the ESACCI data with improved maps of forest areas and harvest is expected to mitigate this source of uncertainty. The forest harvest maps used in our analysis also have uncertainties, which are discussed in Ceccherini et al. (2020), and criticized by Palahí et al. (2021) and Wernick et al. (2021). They mostly concern the inconsistencies of forest change time series and the uncertainty in the algorithm for identifying forest harvest area.

The INVEST model is widely used to simulate the spatial distribution of ESs and the changes over time (Tallis and Polasky, 2009, Posner et al., 2016). The results from INVEST highly depend on the quality of the input datasets and the parameters needed in each module (Sharp et al., 2014). To the best of our knowledge, we used the best available datasets and approaches to quantify key parameters and indicators for the analysis of ESs, and we introduced a transparent procedure for their spatialization (when needed, as for the case of CP and WP) and for the analysis of the synergies and tradeoffs. However, there are some inherent uncertainties in the values used to compile some input tables, such as threat data, biological parameters, and habitat suitability scores (Sharp et al., 2014). These uncertainties will propagate to the simulated ESs. A validation of these input parameters with field observations can reduce their potential uncertainties and achieve more confident results. However, field observations are costly, and usually cover a relatively small area. The possibility to develop hybrid approaches of field observations and satellite retrievals can produce empirical datasets over large areas. Another limitation of INVEST is that snow processes are not considered. This might introduce biases to our simulated ESs, especially those connected to WY and SR. There are available datasets for snow cover, such as the MODIS daily snow cover dataset, but the snow cover has large snow commission error at high altitudes and latitudes (Zhang et al., 2019). Further, explicitly considering snow dynamics and snowfall processes is highly complex, and proper approaches for their inclusion in the evaluation of ESs are missing (Hou et al., 2021).

5. Conclusions

Climate change and anthropogenic activities introduce different impacts on ESs. Understanding the changes of ESs and relationship of each pair of ESs is crucial for a more sustainable management of natural resources. Our study quantitively investigated the ESs in Nordic countries and found out that most of ESs have changed from 2003 to 2018. Both the magnitude of the changes and the relationship between ESs are highly spatially heterogenous. This indicates the need for context-specific measures for landscape management that should consider local conditions, status of ESs, and their individual relationships with the influencing factors.

Currently, we have only studied the pairwise relationship of ESs. A modified approach can extend our framework to the simultaneous analysis of multiple ESs and influencing factors, and the inclusion of spatial explicit yield models might be integrated to ESs assessment so to better capture the influence of changes in climatic conditions and soil erosion on vegetation growth (either trees or crops). Overall, a better understanding of ESs, their dynamics and interlinkage to meteorological and social variables helps to achieving synergies and mitigate tradeoff when deploying more sustainable land use strategies.

CRediT authorship contribution statement

Xiangping Hu: Conceptualization, Methodology, Formal analysis, Writing – original draft, Writing – review & editing, Data curation, Software, Visualization, Investigation. **Yanzhen Hou:** Methodology, Data curation, Formal analysis, Software, Investigation. **Dan Li:** Data curation, Software, Visualization. **Ting Hua:** Methodology, Writing – review & editing. **Maurizio Marchi:** Data curation, Writing – review & editing. **Johana Paola Forero Urrego:** Investigation. **Bo Huang:** Methodology, Investigation, Writing – review & editing. **Wenwu Zhao:** Methodology, Supervision, Funding acquisition. **Francesco Cherubini:** Conceptualization, Methodology, Supervision, Project administration, Funding acquisition, Writing – review & editing.

Declaration of Competing Interest

The authors declare that they have no known competing financial interests or personal relationships that could have appeared to influence the work reported in this paper.

Data availability

Data will be made available on request.

Acknowledgements

Xiangping Hu and Francesco Cherubini acknowledge the support of the Norwegian Research Council (project no. 286773). Yanzhen Hou, Ting Hua and Wenwu Zhao acknowledge support from the National Natural Science Foundation of China (project no. 41861134038) and State Key Laboratory of Earth Surface Processes and Resource Ecology (2022-ZD-08). Bo Huang and Francesco Cherubini acknowledge the support of the Norwegian Research Council (project no. 294534).

References

Bayer, A.D., Fuchs, R., Mey, R., Krause, A., Verburg, P.H., Anthoni, P., Arneth, A., 2021. Diverging land-use projections cause large variability in their impacts on ecosystems and related indicators for ecosystem services. Earth Syst. Dyn. 12, 327–351.
Bennett, E.M., Peterson, G.D., Gordon, L.J., 2009. Understanding relationships among multiple ecosystem services. Ecol. Lett. 12, 1394–1404.
Blanco, V., Holzhauer, S., Brown, C., Lagergren, F., Vulturius, G., Lindeskog, M., Rounsevell, M.D., 2017. The effect of forest owner decision-making, climatic change and societal demands on land-use change and ecosystem service provision in Sweden. Ecosyst. Serv. 23, 174–208.
Borselli, L., Cassi, P., Torri, D., 2008. Prolegomena to sediment and flow connectivity in the landscape: a GIS and field numerical assessment. Catena 75 (3), 268–277.
Bouguerra, S., Jebari, S., 2017. Identification and prioritization of sub-watersheds for land and water management using InVEST SDR model: Rmelriver basin, Tunisia. Arab. J. Geosci. 10, 1–9.
Bradford, J.B., D'Amato, A.W., 2012. Recognizing trade-offs in multi-objective land management. Front. Ecol. Environ. 10, 210–216.
Bryn, A., Potthoff, K., 2018. Elevational treeline and forest line dynamics in Norwegian mountain areas–a review. Landsc. Ecol. 33, 1225–1245.
Cabral, P., Feger, C., Levrel, H., Chambolle, M., Basque, D., 2016. Assessing the impact of land-cover changes on ecosystem services: A first step toward integrative planning in Bordeaux, France. Ecosyst. Serv. 22, 318–327.
Ceccherini, G., Duveiller, G., Grassi, G., Lemoine, G., Avitabile, V., Pilli, R., Cescatti, A., 2020. Abrupt increase in harvested forest area over Europe after 2015. Nature 583, 72–77.
Cord, A.F., Bartkowski, B., Beckmann, M., Dittrich, A., Hermans-Neumann, K., Kaim, A., Lienhoop, N., Locher-Krause, K., Priess, J., Schröter-Schlaack, C., Schwarz, N., Seppelt, R., Strauch, M., Václavík, T., Volk, M., 2017. Towards systematic analyses of ecosystem service trade-offs and synergies: Main concepts, methods and the road ahead. Ecosyst. Serv. 28, 264–272.
Creed, I., Hwang, T., Lutz, B., Way, D., 2015. Climate warming causes intensification of the hydrological cycle, resulting in changes to the vernal and autumnal windows in a northern temperate forest. Hydrol. Process. 29, 3519–3534.
Danielson, J.J., Gesch, D.B., 2011. Global multi-resolution terrain elevation data 2010 (GMTED2010). US Department of the Interior, US Geological Survey Washington, DC, USA.
di Febbraro, M., Sallustio, L., Vizzarri, M., de Rosa, D., de Lisio, L., Loy, A., Eichelberger, B., Marchetti, M., 2018. Expert-based and correlative models to map habitat quality: Which gives better support to conservation planning? Global Ecol. Conserv. 16, e00513.
Dickie, I.A., Yeates, G.W., ST. John, M.G., Stevenson, B.A., Scott, J.T., Rillig, M.C., Peltzer, D.A., Orwin, K.H., Kirschbaum, M.U., Hunt, J.E., 2011. Ecosystem service and biodiversity trade-offs in two woody successions. J. Appl. Ecol. 48, 926–934.
Z. Ding J. Peng S. Qiu Y. Zhao Nearly half of global vegetated area experienced inconsistent vegetation growth in terms of greenness, cover, and productivity. Earth's Future 8 2020 e2020EF001618.
Egoh, B., Reyers, B., Rouget, M., Bode, M., Richardson, D.M., 2009. Spatial congruence between biodiversity and ecosystem services in South Africa. Biol. Conserv. 142, 553–562.
ESA. 2017. *Land Cover CCI: Product User Guide Version 2.0* [Online]. Available: https://maps.elie.ucl.ac.be/CCI/viewer/download/ESACCI-LC-Ph2-PUGv2_2.0.pdf [Accessed May, 27th 2020].
FAO. 2020. *FAOSTAT Datebase* [Online]. Available: http://www.fao.org/faostat/en [Accessed Dec, 12th 2020.
Feng, Q., Zhao, W., Hu, X., Liu, Y., Daryanto, S., Cherubini, F., 2020. Trading-off ecosystem services for better ecological restoration: A case study in the Loess Plateau of China. J. Clean. Prod. 257, 120469.
Feng, Q., Zhao, W., Duan, B., Hu, X., Cherubini, F., 2021. Coupling trade-offs and supply-demand of ecosystem services (ES): A new opportunity for ES management. Geography and Sustainability 2, 275–280.
Filyushkina, A., Strange, N., Löf, M., Ezebilo, E.E., Boman, M., 2016. Non-market forest ecosystem services and decision support in Nordic countries. Scand. J. For. Res. 31, 99–110.
Gorelick, N., Hancher, M., Dixon, M., Ilyushchenko, S., Thau, D., Moore, R., 2017. Google Earth Engine: Planetary-scale geospatial analysis for everyone. Remote Sens. Environ. 202, 18–27.
Haase, D., Schwarz, N., Strohbach, M., Kroll, F., Seppelt, R., 2012. Synergies, trade-offs, and losses of ecosystem services in urban regions: an integrated multiscale framework applied to the Leipzig-Halle Region, Germany. Ecol. Soc. 17.
Hall, L.S., Krausman, P.R., Morrison, M.L., 1997. The habitat concept and a plea for standard terminology. Wildl. Soc. Bull. 173–182.
Hamel, P., Chaplin-Kramer, R., Sim, S., Mueller, C., 2015. A new approach to modeling the sediment retention service (InVEST 3.0): Case study of the Cape Fear catchment, North Carolina, USA. Sci. Total Environ. 524, 166–177.
Hansen, M.C., Potapov, P.V., Moore, R., Hancher, M., Turubanova, S.A., Tyukavina, A., Thau, D., Stehman, S., Goetz, S.J., Loveland, T.R., 2013. High-resolution global maps of 21st-century forest cover change. Science 342, 850–853.
Harfoot, M.B., Johnston, A., Balmford, A., Burgess, N.D., Butchart, S.H., Dias, M.P., Hazin, C., Hilton-Taylor, C., Hoffmann, M., Isaac, N.J., 2021. Using the IUCN Red List to map threats to terrestrial vertebrates at global scale. Nat. Ecol. Evol. 5, 1510–1519.
Hou, Y., Zhao, W., Liu, Y., Yang, S., Hu, X., Cherubini, F., 2021. Relationships of multiple landscape services and their influencing factors on the Qinghai-Tibet Plateau. Landsc. Ecol. 36, 1987–2005.
Hu, X., Huang, B., Verones, F., Cavalett, O., Cherubini, F., 2021a. Overview of recent land-cover changes in biodiversity hotspots. Front. Ecol. Environ. 19, 91–97.
Hu, X.P., Iordan, C.M., Cherubini, F., 2018. Estimating future wood outtakes in the Norwegian forestry sector under the shared socioeconomic pathways. Global Environmental Change-Human and Policy Dimensions 50, 15–24.
Hu, X., Næss, J.S., Iordan, C.M., Huang, B., Zhao, W., Cherubini, F., 2021b. Recent global land cover dynamics and implications for soil erosion and carbon losses from deforestation. Anthropocene 34, 100291.
Hua, T., Zhao, W.W., Liu, Y.X., Wang, S., Yang, S.Q., 2018. Spatial Consistency Assessments for Global Land-Cover Datasets: A Comparison among GLC2000, CCI LC, MCD12, GLOBCOVER and GLCNMO. Remote Sens. 10, 1846.
Hua, T., Zhao, W., Cherubini, F., Hu, X., Pereira, P., 2021. Sensitivity and future exposure of ecosystem services to climate change on the Tibetan Plateau of China. Landsc. Ecol. 36, 3451–3471.
Huang, B., Hu, X.P., Fuglstad, G.A., Zhou, X., Zhao, W.W., Cherubini, F., 2020. Predominant regional biophysical cooling from recent land cover changes in Europe. Nat. Commun. 11, 1–13.
Iordan, C.M., Hu, X., Arvesen, A., Kauppi, P., Cherubini, F., 2018. Contribution of forest wood products to negative emissions: historical comparative analysis from 1960 to 2015 in Norway, Sweden and Finland. Carbon Balance Manag 13, 12.
IPCC 2019. Summary for Policymakers. Climate Change and Land: an IPCC special report on climate change, desertification, land degradation, sustainable land management, food security, and greenhouse gas fluxes in terrestrial ecosystems, J. S. P.R. Shukla, E. Calvo Buendia, V. Masson-Delmotte, H.- O. Pörtner, D. C. Roberts, P. Zhai, R. Slade, S. Connors, R. van Diemen, M. Ferrat, E. Haughey, S. Luz, S. Neogi, M. Pathak, J. Petzold, J. Portugal Pereira, P. Vyas, E. Huntley, K. Kissick, M. Belkacemi, J. Malley. In press.
Larson, M.A., Thompson III, F.R., Millspaugh, J.J., Dijak, W.D., Shifley, S.R., 2004. Linking population viability, habitat suitability, and landscape simulation models for conservation planning. Ecol. Model. 180, 103–118.
Leclère, D., Obersteiner, M., Barrett, M., Butchart, S.H., Chaudhary, A., de Palma, A., Declerck, F.A., di Marco, M., Doelman, J.C., Dürauer, M., 2020. Bending the curve of terrestrial biodiversity needs an integrated strategy. Nature 585, 551–556.
Lehner, B., Grill, G., 2013. Global river hydrography and network routing: baseline data and new approaches to study the world's large river systems. Hydrol. Process. 27, 2171–2186.
Leirpoll, M.E., Næss, J.S., Cavalett, O., Dorber, M., Hu, X., Cherubini, F., 2021. Optimal combination of bioenergy and solar photovoltaic for renewable energy production on abandoned cropland. Renew. Energy 168, 45–56.
Li, W., Ciais, P., Macbean, N., Peng, S.S., Defourny, P., Bontemps, S., 2016. Major forest changes and land cover transitions based on plant functional types derived from the ESA CCI Land Cover product. Int. J. Appl. Earth Obs. Geoinf. 47, 30–39.

Li, W., Macbean, N., Ciais, P., Defourny, P., Lamarche, C., Bontemps, S., Houghton, R.A., Peng, S.S., 2018. Gross and net land cover changes in the main plant functional types derived from the annual ESA CCI land cover maps (1992–2015). Earth Syst. Sci. Data 10, 219–234.
Li, Y., Zhang, L., Qiu, J., Yan, J., Wan, L., Wang, P., Hu, N., Cheng, W., Fu, B., 2017. Spatially explicit quantification of the interactions among ecosystem services. Landsc. Ecol. 32, 1181–1199.
Li, J., Zhou, Z., 2016. Natural and human impacts on ecosystem services in Guanzhong-Tianshui economic region of China. Environ. Sci. Pollut. Res. 23, 6803–6815.
Liang, L., Liu, Q., Liu, G., Li, H., Huang, C., 2019. Accuracy Evaluation and Consistency Analysis of Four Global Land Cover Products in the Arctic Region. Remote Sens. (Basel) 11, 1396.
Liu, X.X., Yu, L., Li, W., Peng, D.L., Zhong, L.H., Li, L., Xin, Q.C., Lu, H., Yu, C.Q., Gong, P., 2018. Comparison of country-level cropland areas between ESA-CCI land cover maps and FAOSTAT data. Int. J. Remote Sens. 39, 6631–6645.
Liu, X., Zhao, W., Liu, Y., Hua, T., Hu, X., Cherubini, F., 2022. Contributions of ecological programs to sustainable development goals in Linzhi, over the Tibetan Plateau: A mental map perspective. Ecol. Eng. 176, 106532.
Lorilla, R.S., Poirazidis, K., Kalogirou, S., Detsis, V., Martinis, A., 2018. Assessment of the spatial dynamics and interactions among multiple ecosystem services to promote effective policy making across mediterranean island landscapes. Sustainability 10, 3285.
Marchi, M., Castellanos-Acuña, D., Hamann, A., Wang, T., Ray, D., Menzel, A., 2020. ClimateEU, scale-free climate normals, historical time series, and future projections for Europe. Sci. Data 7, 1–9.
Marchi, M. 2021. *ClimateDT: Climate Downscaling Tool* [Online]. Available: https://www.ibbr.cnr.it//climate-dt/ [Accessed 2021].
McElwee, P., Calvin, K., Campbell, D., Cherubini, F., Grassi, G., Korotkov, V., le Hoang, A., Lwasa, S., Nkem, J., Nkonya, E., 2020. The impact of interventions in the global land and agri-food sectors on Nature's Contributions to People and the UN Sustainable Development Goals. Glob. Chang. Biol. 26, 4691–4721.
Meijer, J.R., Huijbregts, M.A., Schotten, K.C., Schipper, A.M., 2018. Global patterns of current and future road infrastructure. Environ. Res. Lett. 13, 064006.
Millennium Ecosystem Assessment, M., 2005. Ecosystems and human well-being. Island Press, Washington, DC.
Mouchet, M.A., Lamarque, P., Martín-López, B., Crouzat, E., Gos, P., Byczek, C., Lavorel, S., 2014. An interdisciplinary methodological guide for quantifying associations between ecosystem services. Glob. Environ. Chang. 28, 298–308.
Myers-Smith, I.H., Kerby, J.T., Phoenix, G.K., Bjerke, J.W., Epstein, H.E., Assmann, J.J., John, C., Andreu-Hayles, L., Angers-Blondin, S., Beck, P.S., 2020. Complexity revealed in the greening of the Arctic. Nat. Clim. Chang. 10, 106–117.
Nachtergaele, F., van Velthuizen, H., Verelst, L., Batjes, N., Dijkshoorn, K., van Engelen, V., Fischer, G., Jones, A., Montanarela, L., 2010. The harmonized world soil database 1–6, 34–37.
Palahí, M., Valbuena, R., Senf, C., Acil, N., Pugh, T.A., Sadler, J., Seidl, R., Potapov, P., Gardiner, B., Hetemäki, L., 2021. Concerns about reported harvests in European forests. Nature 592, E15–E17.
Panagos, P., Ballabio, C., Borrelli, P., Meusburger, K., Klik, A., Rousseva, S., Tadić, M.P., Michaelides, S., Hrabalíková, M., Olsen, P., 2015. Rainfall erosivity in Europe. Sci. Total Environ. 511, 801–814.
Panagos, P., 2006. The European soil database. GEO: connexion 5, 32–33.
Pérez-Hoyos, A., Rembold, F., Kerdiles, H., Gallego, J., 2017. Comparison of global land cover datasets for cropland monitoring. Remote Sens. (Basel) 9, 1118.
Posner, S., Verutes, G., Koh, I., Denu, D., Ricketts, T., 2016. Global use of ecosystem service models. Ecosyst. Serv. 17, 131–141.
Qiu, J., Carpenter, S.R., Booth, E.G., Motew, M., Zipper, S.C., Kucharik, C.J., Loheide II, S.P., Turner, M.G., 2018. Understanding relationships among ecosystem services across spatial scales and over time. Environ. Res. Lett. 13, 054020.
Queiroz, C., Meacham, M., Richter, K., Norström, A.V., Andersson, E., Norberg, J., Peterson, G., 2015. Mapping bundles of ecosystem services reveals distinct types of multifunctionality within a Swedish landscape. Ambio 44, 89–101.
Rounsevell, M., Fischer, M., Rando, A. T.-M., Mader, A., Caplat, P., Ekroos, J. & Smith, H. G. 2018. *The IPBES regional assessment report on biodiversity and ecosystem services for Europe and Central Asia*, Intergovernmental Science-Policy Platform on Biodiversity and Ecosystem ….
Sallustio, L., de Toni, A., Strollo, A., di Febbraro, M., Gissi, E., Casella, L., Geneletti, D., Munafò, M., Vizzarri, M., Marchetti, M., 2017. Assessing habitat quality in relation to the spatial distribution of protected areas in Italy. J. Environ. Manage. 201, 129–137.
Samhouri, J.F., Levin, P.S., Ainsworth, C.H., 2010. Identifying thresholds for ecosystem-based management. PLoS One 5, e8907.
Schelhaas, M.-J., Fridman, J., Hengeveld, G.M., Henttonen, H.M., Lehtonen, A., Kies, U., Krajnc, N., Lerink, B., Ní Dhubháin, Á., Polley, H., Pugh, T.A.M., Redmond, J.J., Rohner, B., Temperli, C., Vayreda, J., Nabuurs, G.-J., Hanewinkel, M., 2018. Actual European forest management by region, tree species and owner based on 714,000 re-measured trees in national forest inventories. PLoS One 13 (11), e0207151.
Sharp, R., Tallis, H., Ricketts, T., Guerry, A., Wood, S. A., Chaplin-KRAMER, R., Nelson, E., Ennaanay, D., Wolny, S. & Olwero, N. 2014. InVEST user's guide. *The Natural Capital Project: Stanford, CA, USA.*
Sharpley, A.N., 1990. EPIC-erosion/productivity impact calculator: 1, Model Documentation. USDA Techn. Bull. 1759, 235.
Speed, J.D., Austrheim, G., Kolstad, A.L., Solberg, E.J., 2019. Long-term changes in northern large-herbivore communities reveal differential rewilding rates in space and time. PLoS One 14, e0217166.
Tallis, H., Polasky, S., 2009. Mapping and valuing ecosystem services as an approach for conservation and natural-resource management. Ann. N. Y. Acad. Sci. 1162, 265–283.
Tolessa, T., Senbeta, F., Kidane, M., 2017. The impact of land use/land cover change on ecosystem services in the central highlands of Ethiopia. Ecosyst. Serv. 23, 47–54.
Turner, M.G., Donato, D.C., Romme, W.H., 2013. Consequences of spatial heterogeneity for ecosystem services in changing forest landscapes: priorities for future research. Landsc. Ecol. 28, 1081–1097.
Turner, K.G., Odgaard, M.V., Bøcher, P.K., Dalgaard, T., Svenning, J.-C., 2014. Bundling ecosystem services in Denmark: trade-offs and synergies in a cultural landscape. Landsc. Urban Plan. 125, 89–104.
Vogdrup-Schmidt, M., Olsen, S.B., Dubgaard, A., Kristensen, I.T., Jørgensen, L.B., Normander, B., Ege, C., Dalgaard, T., 2019. Using spatial multi-criteria decision analysis to develop new and sustainable directions for the future use of agricultural land in Denmark. Ecol. Ind. 103, 34–42.
Werner, B.A., Johnson, W.C., Guntenspergen, G.R., 2013. Evidence for 20th century climate warming and wetland drying in the North American Prairie Pothole Region. Ecol. Evol. 3, 3471–3482.
Wernick, I.K., Ciais, P., Fridman, J., Högberg, P., Korhonen, K.T., Nordin, A., Kauppi, P. E., 2021. Quantifying forest change in the European Union. Nature 592, E13–E14.
Winkler, A.J., Myneni, R.B., Hannart, A., Sitch, S., Haverd, V., Lombardozzi, D., Arora, V. K., Pongratz, J., Nabel, J.E., Goll, D.S., 2021. Slowdown of the greening trend in natural vegetation with further rise in atmospheric CO 2. Biogeosciences 18, 4985–5010.
Wiréhn, L., 2018. Nordic agriculture under climate change: A systematic review of challenges, opportunities and adaptation strategies for crop production. Land Use Policy 77, 63–74.
Yin, C., Zhao, W., Cherubini, F., Pereira, P., 2021. Integrate ecosystem services into socio-economic development to enhance achievement of sustainable development goals in the post-pandemic era. Geogr. Sustain. 2, 68–73.
Yue, D., Zhou, Y., Guo, J., Chao, Z., Liang, G., Zheng, X., 2022. Ecosystem service evaluation and optimisation in the Shule River Basin, China. *CATENA* 215, 106320.
Zhang, L., Hickel, K., Dawes, W., Chiew, F.H., Western, A., Briggs, P., 2004. A rational function approach for estimating mean annual evapotranspiration. Water Resour. Res. 40.
Zhang, H., Zhang, F., Zhang, G., Che, T., Yan, W., Ye, M., Ma, N., 2019. Ground-based evaluation of MODIS snow cover product V6 across China: Implications for the selection of NDSI threshold. Sci. Total Environ. 651, 2712–2726.
Zhou, N., Hu, X., Byskov, I., Næss, J.S., Wu, Q., Zhao, W., Cherubini, F., 2021. Overview of recent land cover changes, forest harvest areas, and soil erosion trends in Nordic countries. Geogr. Sustain. 2, 163–174.
Zhu, Z.C., Piao, S.L., Myneni, R.B., Huang, M.T., Zeng, Z.Z., Canadell, J.G., Ciais, P., Sitch, S., Friedlingstein, P., Arneth, A., Cao, C.X., Cheng, L., Kato, E., Koven, C., Li, Y., Lian, X., Liu, Y.W., Liu, R.G., Mao, J.F., Pan, Y.Z., Peng, S.S., Penuelas, J., Poulter, B., Pugh, T.A.M., Stocker, B.D., Viovy, N., Wang, X.H., Wang, Y.P., Xiao, Z. Q., Yang, H., Zaehle, S., Zeng, N., 2016. Greening of the Earth and its drivers. Nat. Clim. Chang. 6, 791–795.